ICHE 2014, Hamburg - Lehfeldt & Kopmann (eds) - © 2014 Bundesanstalt für Wasserbau ISBN 978-3-939230-32-8

# A Laboratory Study for Gravity Erosion of the Steep Loess Slopes under Intense Rainfall

X.-Z. Xu & C. Zhao
*School of Hydraulic Engineering, Dalian University of Technology, Dalian, China*

ABSTRACT: Gravity erosion is a common and destructive phenomenon in mountainous areas throughout the world, especially on the Loess Plateau of China. This study closely simulates the gravity erosion processes of 7 model slopes with different slope gradients and heights, and quantitatively observes the amounts of collapse, landslide, and mudflow, respectively. Erosion data during rainfall event were calculated according to the videos caught by the Topography Meter. The experimental result is shown as follows: 1) The form of the gravity erosion was decided by the slope gradient of the gully wall. For the initial slope with same height but different gradient, when the slope became precipitous, the amount of collapse might grow and the amount of landslide might decrease. 2) For the slopes with the same height, the amount of collapse increased with the enlargement of the slope gradient, but the amounts of landslide and the total gravity erosion were different. 3) For the slopes with the same slope gradient, the amount of collapse increased with the enlargement of the slope height, but the amounts of landslide and the total gravity erosion were different. 4) As the loess gully wall is eroding, the amount of gravity erosion was jointly impacted by the water content and the landform.

*Keywords: Slope landform, Landslide volume, Topography Meter, Laboratory test*

## 1 INTRODUCTION

Gravity erosion, also referred as gravitational erosion or mass erosion, is a mass failure on steep slopes caused by the self weight of the soil, in contrast to other erosions induced by the physical forces, e.g. wind water. On the Loess Plateau of China, there are various types of gravity erosion, including landslide, land avalanche, earth flow, creep, etc (Tang et al 2004). Gravity erosion usually takes place accompanied with water erosion during rainfall events, while the mechanisms and dynamics are markedly different. Therefore, to set up mechanical models for gravity erosion, water erosion included in the landslide must be removed. Yet predicting just where and when a mass failure will occur is always a complicated issue. No direct observation of the soil geotechnical parameters at failure moment for any specific site has ever been recorded.

A variety of techniques have been used to estimate the gravity erosion, each with its own intrinsic limitations and uncertainties. Earlier approaches basically focused on the qualitative relationship between the gravity erosion in the upper reach and the hyperconcentrated flow in the alluvial river (e.g., Wang et al. 1982). By integrating the complete response of the observation system, Hovius et al. (1997) found that sediment discharge from the western Southern Alps was dominated by landslide-derived material. In recent years, remote sensing technologies, e.g. terrestrial laser scanning (Oppikofer et al. 2008), sonar bathymetry (Haflidason et al. 2005), radar altimetry (Velicogna and Wahr 2006), aerial photograph (Whitehouse 1983; Martin et al. 2002), have been used to monitor soil erosion and geomorphic evolution. But the fact is that it is very difficult to record the time-variable process with these technologies because of the randomness of an individual landslide. A strain probe method was developed to continuously measure the soil creep in situ and preestimate the volume of slope failure (Yamada, 1999; Iverson et al. 2000). The tracer element method is also a helpful approach (Wen et al. 2003). Despite all these, it is still not possible to differentiate the soil volume of gravity erosion from water erosion.

The volume of an individual mass failure was normally calculated by multiplying the slide area by the slide thickness. Sattar et al. (2011) determined the dimensions of an eroded gully with a laser scanner, and revealed the soil volume and the volume change in the landslide dam body. Many other studies on individual measurement of landslide area and soil volume for multiple slope failures in certain areas were also carried out (e.g., Whitehouse 1983; Derbyshire et al. 1995; Larsen and Torres-Sanchez 1998; Martin et al. 2002; Haflidason et al. 2005; Guzzetti et al. 2009; Jaiswal et al. 2011).

The Loess Plateau is located in the upper and middle reaches of the Yellow River (Figure. 1), covering a total area of 624,000 $km^2$, and over 60% of the land is subjected to serious soil and water loss. Gravity erosions are the major soil source for small watershed (Xue et al. 2009). Among them, small erosion within seveal decimeters in depth occurs most frequently, and it has a huge influence on the sediment yield for the river basin (Cai 1993). However, systematic observation, measurement, and experiment were still absent due to the complexity of gravity erosion. Wang et al. (1982) and Zhang et al. (2006) have analyzed the runoff via actual measurements at the monitoring stations. The total amount of gravity erosion was also calculated with geometry measurements (e.g., Ye 2004). Xu et al. (1999) has explored the collapse mechanism of a river bank and estimated the landslide volume according to the erosion scope during a model test.

Aiming at further investigate the occurrence mechanism of gravity erosion on the Loess Plateau, this study set up a generalized model with various slope gradient and slope length in the laboratory. Integrated behaviors on a small event were studied via a series of rainfall simulation experiments. Dynamic and quantitative observations on the full course of gravity erosion were measured by the MX-2010-G Topography Meter invented by the authors of this paper (Zhao et al. 2011).

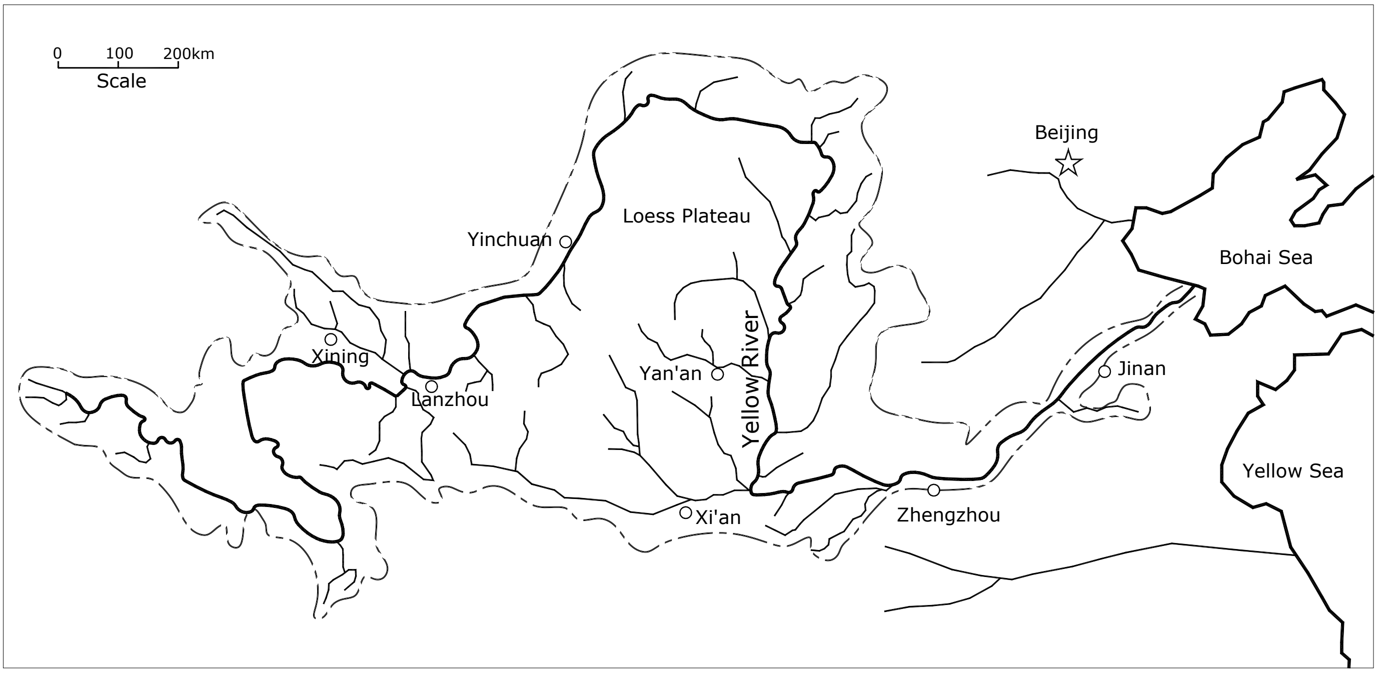


Figure 1. A sketch map of the Loess Plateau of China.

## 2 EXPERIMENTAL SETUP AND METHODS

The experiments were conducted in the Joint Laboratory for Soil Erosion of Dalian University of Technology and Tsinghua University under closely controlled conditions. 7 groups of terrain were constructed, each undergoing 6-10 rainfalls with a duration time of 30 min. The rain intensity was 2.0 mm/min, approximately identical to the Type A rainstorm on the Loess Plateau. The rainfall interval is 24 h. The experiment ceased when the slope gradually becomes lower and the erosion amount of rainfall reduced until to a certain value. Then new landscape will be built for the next experiment. The simulated rainfall times was determined by the extent of the fragmentation, probability of gravity erosion occurrence and water content in the soil of the terrain.

The landscape simulator consisted of a rainfall simulator suspended above a flume containing the slope model, as shown in Figure 2. Six lines of five sprayer-styled rainfall simulators were utilized to simulate rainfall in the experimental plot covering 3.0×3.0 meters. A short and intense downpour, with an intensity of 2.0 mm/min and the duration of 30 min, was applied. The landscape was constructed using matrix loess collected from the Shunyi District, Beijing. The 50% diameter of soil particles, D50, was 52.2 μm, and specific gravity, γs, was 2.56. An experimental model landscape, with the steep slope of 60 - 80$^o$ and a gentle slope of 3$^o$, was developed. Soil was prepared by hand patting to generate a 'smooth' roughness to ensure a regular and original microrelief. 6 - 10 rainfalls were applied on the slope in turn. Roughly equal interval, 12 hours or so, was kept after each rainfall. Then new landscape was built for the next experiment.

Dynamic variations of steep slopes were monitored by the Topography Meter under simulated rainfalls. Volume of an individual failure mass was assessed by comparing the failure block geometry just before and after the incident. The hardware components of a Topography Meter consist of a number of regular devices: a video, a laser source, and a position device. A stripe pattern with equidistant horizontal lines is generated by the laser source, and will be recorded by the camera with sighting direction perpendicular to the light pattern. Positioning marks are placed on the fixed position with same height. As the slope terrain deforms over time, video of the changing process will be recorded and imported into the computer to acquire snapshot images at particular time instances. Given depth in ArcGIS, the 3D geometric shape of the target surface can be computed accurately. The laboratory calibration tests on the wooden brae show that all the relative errors of the observed volumes were within 10% for the five landform models with the total soil volume of about 24,000 cm$^3$ and slope gradients of 35 - 75$^o$ (Zhao et al., 2011). Subsequent slumps will continue after the rainfall. Therefore, the total failure volume of a rainfall was calculated by comparing the slope volume at the end of the rainfall with that at the beginning of the next rainfall.

The water content in the underlying surface was detected by a RR-1008 Water Monitor every 30 sec. 5 sensor probes were embedded from the top down the model with a vertical interval of 1/10 the total height, as illustrated in Figure 2.

Three gravity erosions happened in the experiments in form of landslide, collapse and mudslide. Since mudslide has a relatively small amount, we will investigate the erosion of landslide and collapse only. The phenomenon that rock soil on the slope moves down as a whole along a certain weak belt or surface is called landslide, while that rock soil suddenly topples, fragments and rolls down a slope face is termed collapse. Mass movement, or original lithology is a key characteristics of landslide.

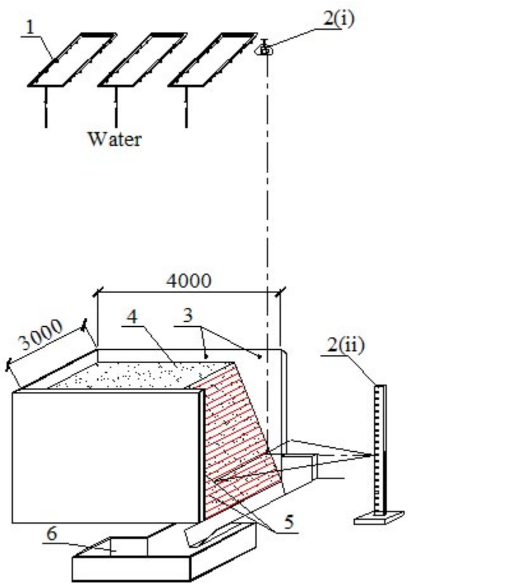


Figure 2. Schematic diagram of the model experiment. Key: 1 Rainfall simulator; 2 Topography Meter (i. Video with a collimator; ii. Laser source); 3 Positioning marks; 4 Model slope; 5 Equidistant horizontal projections; 6 Runoff pool.

## 3 RESULTS AND DISCUSSION

The effects of water content in the underlying surface, slope gradient and degree of landscape crushing on the gravitational erosion were analyzed via comparing the previous erosion amounts on the same initial landform, whereas the effect of slope gradient and slope height were analyzed via comparing the average erosion amounts on the same initial landform.

### 3.1 *Partial correlation analysis between gradient and height of the slope and gravitational erosion*

Partial correlation analysis between total erosion amount, collapse amount, landslide amount of each rainfall and gradient and height of the slope was made on all the 48 rainfalls over different slope gradients and slope heights, as shown in Table 1. All have passed the significance test. When the slop height was set, the partial correlation coefficient of gravity erosion, land avalanche and slope gradient were 0.181 and 0.280 separately. This indicates that the event collapse amount and gravity erosion amount increased with the slope gradient, especially the former. The coefficient of partial correlation between landslide and slope gradient was -0.162, indicating that the landslide amount tended to reduce at the steep slope over 60$^o$. On the other hand, when the slop gradient was set, the partial correlation coefficient of gravity erosion, land avalanche, landslide and slop height were 0.162, 0.143 and 0.065. Landslide had the minimum partial correlation coefficient, accounting for the less effect of slope height. Collapse had the maximum partial correlation coefficient in both cases, illustrating the sensitivity of the variable. Detailed analysis will be continued in the rainfall test.

Table 1. Partial correlation analysis of the slope height and gradient on the gravity erosion

| Variable | Slope gradient | | Slope height | |
|---|---|---|---|---|
| | Relevance | significance | Relevance | significance |
| Gravity erosion | 0.181 | 0.209 | 0.162 | 0.262 |
| Land avalanche | 0.280 | 0.049 | 0.143 | 0.322 |
| Landslide | -0.162 | 0.260 | 0.065 | 0.656 |

### 3.2 *The effect of slope gradient on gravity erosion*

The severity of slope has an important effect on gravity erosion. When the gradient continually increased, gravity erosion will change from landslide to collapse. Table 2 displayed the average erosion amounts for all rainfall events. Landslide is the main erosion for the relatively gentle slope of 60$^{o}$, which erosion amount accounts for 60.0~76.2%. In contrast, collapse becomes the predominate erosion for the steep slope of 70$^{o}$ and 80$^{o}$, making up 77.6~89.6% of the total erosion.

Table 2. Relationship of the average landslide amount among the height and the slope gradient for all rainfall events on an initial landform

| Erosion amount | Initial slope | Erosion style | Collapse (C) | | Landslide (S) | | Total (G) | |
|---|---|---|---|---|---|---|---|---|
| | | Height (m) | 1.0 | 1.5 | 1.0 | 1.5 | 1.0 | 1.5 |
| Gravity erosion /($10^{-3}m^3$) | 60° | | 13.8 | 21.0 | 44.1 | 31.6 | 57.9 | 52.6 |
| | 70° | | 24.1 | 68.6 | 2.8 | 15.8 | 26.9 | 84.3 |
| | 80° | | 63.4 | 74.9 | 12.4 | 21.6 | 75.8 | 96.5 |
| Ratio of the collapse or landslide to the total /% | 60° | | 23.8 | 40.0 | 76.2 | 60.0 | —— | —— |
| | 70° | | 89.6 | 81.3 | 10.4 | 18.7 | —— | —— |
| | 80° | | 83.7 | 77.6 | 16.3 | 22.4 | —— | —— |
| Increase as the gradient a/% | 60° | | —— | —— | —— | —— | —— | —— |
| | 70° | | 74.7 | 225.8 | -93.7 | -50.0 | -53.6 | 60.3 |
| | 80° | | 163.4 | 9.3 | 342.2 | 37.1 | 182.0 | 14.5 |
| Increase as the height b/% | 60° | | —— | 52.8 | —— | -28.4 | —— | -9.1 |
| | 70° | | —— | 184.9 | —— | 463.8 | —— | 213.9 |
| | 80° | | —— | 18.2 | —— | 74.8 | —— | 27.4 |

* Notes: Increase of the erosion as the slope gradient rose: $a=(g_2-g_1)/g_1\times100\%$, where $g_1$ is the amount of collapse, landslide, or total gravity erosion for a certain landform, and $g_2$ is the erosion amount of the landform with the same height but the slope gradient increased 10$^{o}$; increase of the erosion as the slope gradient rose: $b=(g_3-g_1)/g_1\times100\%$, where $g_3$ is the erosion amount of the landform with the same gradient but the slope height increased 0.5 m.

For different initial landform, slope gradient affects the collapse amount most, whereas it has less effect on landslide amount and total collapse amount. Slope height also has less effect on above parameters. Taken the 1.0m landform in Table 2 as an example, when the initial gradient increased from 60° to 70°, the collapse amount increased 74.7%, landslide amount decreased 93.7%, and the total erosion decreased 53.6%; while when the initial gradient increased from 70° to 80°, the collapse amount increased 163.4%, landslide amount increased 342.2%, and the total erosion increased 182.0%.

For the same initial landform, the slope becomes more and gentler with rainfalls, which means landslide erosion increases and collapse erosion decreases. Table 2 reveals mass failure amount in rainfall event. For the slope with an initial gradient over 60° and slope height of 1.0 m, collapse was the main erosion for the 1-4 rainfalls, and landslide became crucial for the 5-7 rainfalls. While for the slope with an initial slope height of 2.0 m, collapse was the main erosion for the 1-5 rainfalls, and landslide ranked first for the 6-10 rainfalls. These phenomena reflected the important role of water erosion. In the first several rainfalls, the slope is quite steep and upper soil mass is easy to collapse under the washing of the rain.

While after some rainfalls, the slope becomes stable and the gradient turns gentle, which is benefit for the landslide to take place. Especially for the relative gentle landform with a gradient of 60° and height of 1.0m, landslide is dominated in all the six rainfalls. These results is consistent with the remote-monitored tests of Wang et al (2001).

In summary, on the steep slope, e.g. 70°~80° in our study, collapse is the leading erosion type, varied sensitively with the slope gradient.

### 3.3 *The effect of slope height on gravity erosion*

Collapse is a high-speed movement of the soil mass cracked from the ground, dumped to the free surface, and torn instantly from their parent. Therefore, the potential energy of a collapsed mass has a direct impact on the erosion amount. But the potential energy depends on the volume and height of the collapsed mass; hence the effect of slope height on erosion is significant. In contrast, landslide is a soil slide under gravity along the slope. Its potential energy was weakened by the friction of slope, so the influence of the slope height is relatively small.

Table 2 lists the average erosion amount of rainfalls. It can be seen that collapse amount, landslide amount and the total erosion amount all increases with the slope height. When the slope height increases from 1.0m to 1.5m, the collapse amounts increase 52.8%, 184.9% and 18.2% on the landform of 60 $^{o}$, 70$^{o}$ and 80 $^{o}$ separately. But the landslide amount and the total erosion amount varied, e.g., they increased to 463.8% and 213.9% for the landform of 70 $^{o}$, and decreased to28.4% and 9.1% for the landform of 60 $^{o}$. The test results approve that, the collapse amount is significantly affected by the slope height, whereas the slope gradient and slope height has less effect on the landslide amount and the total erosion amount.

The effluence of slope height on erosion can be also obtained by comparing the erosion amount of every rainfall at the same slope gradient and different slope height. Table 2 exhibits the erosion amounts of every rainfall at slope height of 1.0m, 1.5m and 2.0m and gradient of 70 $^{o}$. It can be observed that the erosion amount of 1.5m landform is much larger than that of 1.0m, though the overall amount of all erosions is approximately the same. But when the slope height is 2.0m, the increase in the total erosion amount is quite significant. Especially for the 5th rainfall, the landslide amount and the total erosion amount reached $763.6\times10^{-3}m^3$ and $767.2\times10^{-3}m^3$, indicating the obvious increase in the danger of erosion.

### 3.4 *The combined effect of water content in the underlying surface, gully density and slope gradient on the gravity erosion*

Water content in the slope and degree of crushing of the surface are also main natural factor for the stability of slope. In China, most landslides were aroused by the change of underground water arisen from rainfalls. The soil will absorb water to gain weight and expand volume, till the balance is destroyed to collapse or landslide. Therefore, water content is an internal factor to gravity erosion. The effect of degree of crushing of the surface on gravity erosion is complicated. It was found in the previous experiments that smooth and neat landform is highly-resistant to gravity erosion. Local water content may increase rapidly and collapse when pit, hollow and erosion gully occurred on the slope. But when small erosion gully were converged to a lateral erosion gully, where most rain will flow through, slump is difficult to happen on both side of the slope due to the gully head control formed by erosion. When the erosion further continued, some slope will separate from the surface and caused gravity erosion.

Figure 3 depicts the three stages of gravity erosion after rainfalls. In the first stage, the slope is neat and smooth, the water content is unsaturated, and the possibility of gravity erosion is very small. In the second stage, water content in the underlying layer continued to rise, and the slope surface broke gradually resulting from interactions of gravity and water. Gravity erosion occurs frequently and the amount is very large. In the third stage, the slope is relatively gentle, the breakage of the landform has reached a limit, and water content approaches each other, in the range of 20.1%~32.0%. Erosion amount of every rainfall gets small. In view of these, it can be concluded that the gravity erosion amount of every rainfall is some contribution of water content, slope gradient, degree of surface crushing, etc.

# 4 CONCLUSIONS

The following main conclusions were drawn from the present study:

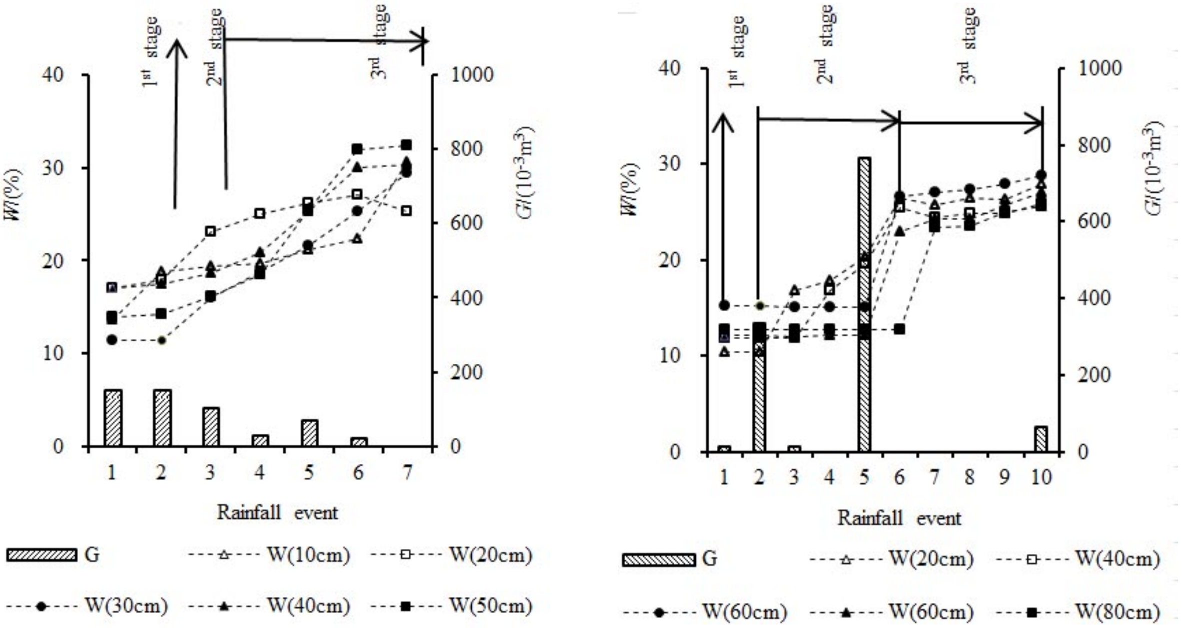


(a) Slope height was 1.5m and gradiengt was 60°

(b) Slope height was 1.0 m and gradiengt was 80°

Figure 3. Water content and gravity erosion of each rainfall event on a landform.

1) The form of the gravity erosion was decided by the slope gradient of the gully wall. For the initial slope with same height but different gradient, when the slope became precipitous, the amount of collapse might grow and the amount of landslide might decrease. Especially when the slope gradient was between 70° and 80°, the amount of gravity erosion would be more sensitive to the slope gradient.
2) For the slopes with the same height, the amount of collapse increased with the enlargement of the slope gradient, but the amounts of landslide and the total gravity erosion were different. For the slope with the height of 1.0 m, when the slope gradient rose from 60° to 70°, the amounts of collapse, landslide, and the total gravity increased 74.7%, -93.7%, and -53.6%, respectively. Nevertheless, when the slope gradient rose from 70° to 80°, the amounts of collapse, landslide, and the total gravity increased 163.4%, 342.2%, and 182.0%, respectively.
3) For the slopes with the same slope gradient, the amount of collapse increased with the enlargement of the slope height, but the amounts of landslide and the total gravity erosion were different. When the slope height rose from 1.0m to 1.5m, for the slopes with the gradients of 60°, 70°, and 80°, the amounts of collapse increased 52.8%, 184.9%, 18.2%, the amounts of collapse increased -28.4%, 463.8%, 74.8%, the amounts of collapse increased -9.1%, 213.9%, 27.4%, respectively.
4) As the loess gully wall is eroding, the amount of gravity erosion is jointly impacted by the water content and the landform. The latter includes the slope gradient, height, and broken degree, etc.


## ACKNOWLEDGEMENTS

This study is supported by the Open Research Fund Program of Key Laboratory of Process and Control of Soil Loss on the Loess Plateau (2014001) and the National Natural Science Foundation of China (51179021; 51079016). Sincere thanks are also given by the first author to Professor Yu Cong for amending English writing.


## REFERENCES


Cai, Q.G. (1993). Ratio and law of the sediment transportation in the gully, in: Chen H., Soil loss on the catchment slope and gully. China Meteorological Press, Beijing, China, pp224 (in Chinese)

Derbyshire E., Asch T.V., Billard A., Meng X. (1995) Modelling the erosional susceptibility of landslide catchments in thick loess: Chinese variations on a theme by Jan de Ploey. Catena 25: 315-331

Guzzetti F., Ardizzone F., Cardinali M., Rossi M. and Valigi D. (2009) Landslide volumes and landslide mobilization rates in Umbria, central Italy. Earth Planet Sc Lett 279: 222–229
Haflidason H., Lien R., Sejrup H.P., Forsberg C.F., Bryn P. (2005) The dating and morphometry of the Storrega Slide. Mar Petrol Geol 22: 187–194.
Hovius N., Stark C.P., Allen P.A. (1997) Sediment flux from a mountain belt derived by landslide mapping. Geology 25: 231–234
Iverson R.M., Reid M.E., Iverson N.R., LaHusen R.G., Logan M., Mann J.E., Brien D.L. (2000) Acute sensitivity of landslide rates to initial soil porosity. Science 290: 513–516
Jaiswal P., Westen C.J., Jetten V. (2011) Quantitative assessment of landslide hazard along transportation lines using historical records. Landslides 8: 279–291
Larsen M.C., Torres-Sanchez A.J. (1998) The frequency and distribution of recent landslides in three montane tropical regions of Puerto Rico. Geomorphology 24: 309–331
Martin Y., Rood K., Schwab J.W., Church M. (2002) Sediment transfer by shallow landsliding in the Queen Charlotte Islands, British Columbia Canadian. J Earth Sci 39: 189–205
Oppikofer T., Jaboyedoff M., Keusen, H.-R. (2008) Collapse at the eastern Eiger flank in the Swiss Alps. Nature Geosci 1: 531–535.
Tang K.L. (2004) Soil and water conservation in China. Science Press, Beijing (in Chinese)
Velicogna I., Wahr J. (2006) Measurements of time-variable gravity show mass loss in Antarctica. Science 311: 1754
Wang J., Yang X., Ni J. (2001) GIS supported study on gravitational erosion distribution——case of the catchments of the middle reach of Yellow River, Journal of Basic Science and Engineering, 9(1): 23—32. (in Chinese)
Wang X.K., Qian N., Hu W.D. (1982) The formation and process of confluence of the flow with hyperconcentration in the Gullied-hilly Loess areas of the Yellow River Basin. J Hydraul Eng (7): 26–35 (in Chinese)
Wen A.B., Zhang X.B., Zhang Y.Y., Xu J.Y., Bai L.X. (2003) Comparison study on sediment sources between debris flow gullies and non-debris flow gullies by using the 137Cs tracing technique in Dongchuan, Yunnan Province of China. J Sediment Res (4): 52–57 (in Chinese)
Whitehouse I.E. (1983) Distribution of large rock avalanche deposits in the Central Southern Alps, New Zealand. J Geol Geop 26: 271–279
Xu Y., Kuang S., Li W., (1999) et al. Effects of slope shape on avalanches, Journal of Sediment Research, (5): 67—73. (in Chinese)
Xue H. (2009) Wang G., Li T. Review of gravitational erosion researches in the middle reach of Yellow River [J], Advances in Water Science, 20(4): 599—606. (in Chinese)
Yamada S. (1999) The role of soil creep and slope failure in the landscape evolution of a head water basin: field measurements in a zero order basin of northern Japan. Geomorphology 28: 329–344
Ye H. (2004) Mechanism of pi-sandstone gravity erosion and its evaluation in the Transition Zone between Shaanxi and Neimeng, Middle Reaches of Yellow River [D], Chinese Academy of Geological Sciences, Zhengding, China. (in Chinese)
Zhang L., Wang S., Wang J., et al. (2006) Analysis on characteristics of soil and water loss of Luergou watershed in Gullied Rolling Loess Area, Yellow River, 28(12): 49—5. (in Chinese)
Zhao C., Xu X., Xu F., Wang S. (2011) A device to measure dynamic process of slope erosion. Science of Soil and Water Conservation, 10(1): 65—69. (in Chinese)